

## Ionospheric Electron Content and Variations Measured by Doppler Shifts in Satellite Transmissions<sup>1</sup>

FERNANDO DE MENDONÇA

*Radioscience Laboratory, Stanford University, Stanford, California*

**Abstract.** A method is derived for calculating ionospheric electron content by comparison of the Doppler shifts imparted to two harmonically related frequencies transmitted from a satellite. This Doppler method is applied in the analysis of many passages of the satellite Transit 2-A (1960<sub>71</sub>) during the months of July through October 1960. The observations were made at Stanford, California, on the frequencies of 54 Mc/s and its sixth harmonic. Differences in the electron content of 25 per cent between two subionospheric points separated by as little as 1000 km were observed on several passages during magnetically quiet days. On some magnetically disturbed days these differences increased to over 50 per cent for the same separation. A very strong magnetic storm is shown to decrease the early-afternoon electron content to almost a normal nighttime value over the range of latitudes surveyed. Other less intense storms are observed to decrease the electron content to the north and to increase it to the south of the observer. The day-to-day variations of electron content at a given latitude on magnetically quiet days are observed to be about  $\pm 15$  per cent from the mean; however, less frequently, variations as large as  $\pm 50$  per cent were observed. Unlike the variations on the magnetically disturbed days, these variations did not seem to modify the horizontal gradients normally found.

### INTRODUCTION

One of the most straightforward and powerful methods of studying the ionosphere is by means of measurement of the total electron content or the columnar density. For these measurements, satellite transmissions are at present one of the best sources of data. Basically two types of measurements can be made with satellite signals for the purpose of determining electron content, namely, Faraday and Doppler techniques.

Garriott [1960], using the Faraday effect in two different approaches (polarization-rotation-angle and polarization-rotation-rate measurements), analyzed several months of data obtained by recording the 20 and 40 Mc/s signals radiated from the satellite 1958<sub>8</sub> (Sputnik 3). Yeh and Swenson [1961], using signals from the same satellite, also developed a procedure for correcting the effect of refraction and the high-frequency approximation when Faraday rotation rate measurements are used.

Doppler techniques have been used in the study of the ionosphere either with transmissions from rockets [Nisbet and Bowhill, 1960; Seddon, 1953] or from satellites [Weekes, 1958; Hibberd and Thomas, 1959; Aitchinson and Weekes, 1959; Ross, 1960; Garriott and Nichol, 1961]. In this paper, we are concerned with the method in which CW signals are propagated between a moving transmitter and an observer at two harmonically related frequencies. Because of ionospheric dispersion, the lower frequency has a much larger change in phase than the higher frequency. Thus, when satellite signals are properly detected in phase-locked systems, we can measure the time rate of change of the relative phases and obtain information about the ionospheric electron content and its spatial variations.

For satellites in circular orbits, we obtain measurements that can be processed to give us the equivalent columnar electron density; for those in elliptical orbits, the presence of a vertical component of velocity will add information about the electron density at the satellite. We must be aware that the columnar electron density is measured along an oblique line from the observer to the satellite and is transformed to an equivalent columnar density by means of a

<sup>1</sup>This paper was presented at the joint meeting of the International Scientific Radio Union (URSI) and of the Institute of Radio Engineers held October 24, 1961, at the University of Texas, Austin, Texas.

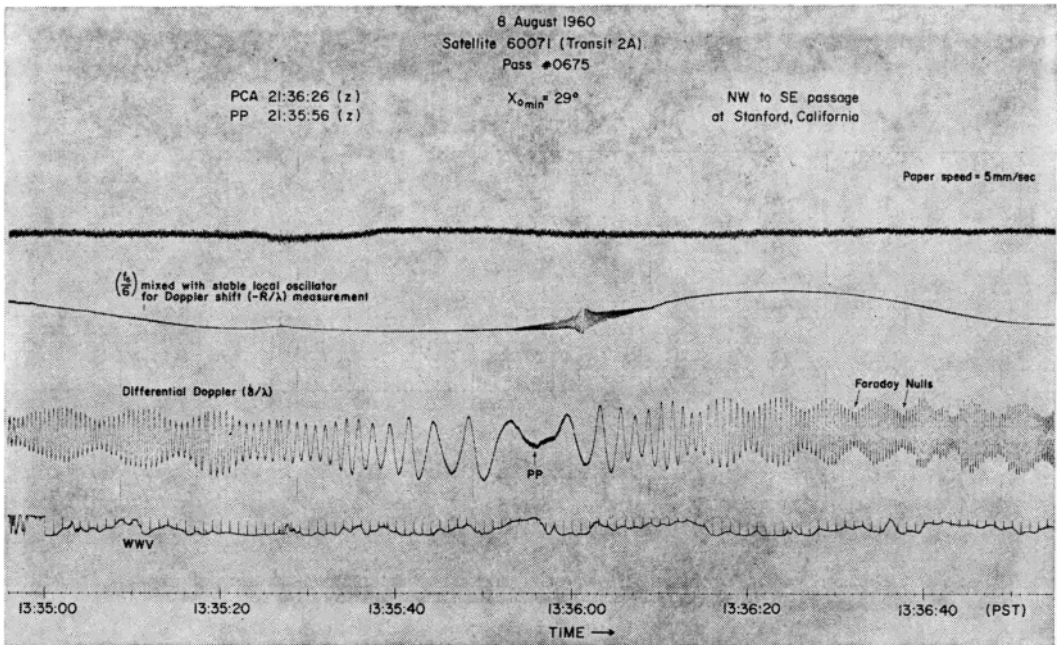


Fig. 1. Differential Doppler ( $\delta/\lambda$ ) for an afternoon passage of satellite Transit 2-A with proximal point PP 30 sec earlier than the point of closest approach PCA.  $h_e(0) = 730$  km;  $\dot{h}_e(t_c) = -223$  m/sec.

geometrical factor. For the sake of simplicity, we shall call it columnar density. Initially, we will use all the quantities involved as functions of time, transforming them later into functions of position by means of the satellite's ephemerides. The origin of our relative time will be the time at which the satellite reaches the geometrical point of closest approach (PCA), that is, the point at which the first derivative of the range  $R$  with respect to time is zero. Another point of interest for every passage is the point at which the difference between range and phase path between observer and satellite reaches a minimum. It is called the proximal point (PP) and is characterized by the fact that then the first derivative of the phase path defect ( $\Delta P$ ) with respect to time is zero. Normally, because of the presence of vertical velocities, horizontal gradients, tilts, and other irregularities in the electron distribution, these two points, PCA and PP, do not coincide. It is essential that they be accurately determined, because their separation greatly influences the resultant measurement.

The method of analysis in this paper has been derived primarily to use data from satellites of the Transit series, which transmit a pair of

harmonically related frequencies, 54 and 324 Mc/s. These satellites have been planned for navigational purposes, but they have also been found most useful for the deduction of ionospheric information. With trivial modifications the process can be used with other frequencies.

If we assume that, at the level of the  $F$  region, the collisional frequency is negligible and the gyrofrequency  $f_H$  and plasma frequency  $f_p$  are much smaller than the fundamental frequency  $f$  of the harmonically related pair, then we may write the refractive index of the medium as

$$\mu \approx 1 - (K_1/2f^2)N \quad (1)$$

where  $N$  is the electron density and  $K_1$  is a constant (80.6 mks units).

Later we shall discuss the errors introduced by the assumptions above.

#### THEORY

To find an exact solution for the propagation problem in the satellite-observer medium is a task of considerable difficulty. It is imperative to make adequate approximations to allow calculation of the electron content from the Dop-

pler measurements. Having outlined our assumptions about frequencies used and restricting ourselves to observations where the zenith angle  $\chi_m$  is smaller than  $60^\circ$ , we can disregard the influence of large refractive effects, as will be shown later, and write the following expression for the range  $R$  between the observer and the satellite:

$$R = \int_0^s ds \tag{2}$$

Without any approximation, the phase path  $P$  is given by

$$P = \int_0^s \mu ds \tag{3}$$

Their difference in length is called *phase path defect* [Garriott and Bracewell, 1961]:

$$\Delta P = R - P = \int_0^s (1 - \mu) ds \tag{4}$$

and using (1) we write

$$\Delta P = \frac{K_1}{2f^2} \int_0^s N ds \tag{5}$$

If we now consider the  $n$ th harmonic as the higher frequency that will also be received, we can write the difference

$$\begin{aligned} \delta &= (\Delta P - \Delta P_n) \\ &= \left[ \frac{1}{f^2} - \frac{1}{(nf)^2} \right] \frac{K_1}{2} \int_0^s N ds \end{aligned} \tag{6}$$

or

$$\delta = \left[ \frac{n^2 - 1}{n^2} \right] \frac{K_1}{2f^2} \int_0^s N ds \tag{7}$$

Then

$$\Delta P = n^2 / (n^2 - 1) \delta \tag{8}$$

In the acquisition of data using phase-locked receivers, we actually measure the beat between the fundamental frequency  $f$  and the frequency ( $f_n/n$ ) after they have been subjected to the dispersive effects of the ionosphere. This beat, displayed in Figure 1, from a particular satellite passage is called *differential Doppler* and is equal to the time rate of change of the quantity  $\delta$ , shown in (7), divided by the free-space wavelength  $\lambda$  of the fundamental signal. Differen-

tiating (8) with respect to time we obtain

$$\left( \frac{\Delta \dot{P}}{\lambda} \right) = \frac{n^2}{n^2 - 1} \left( \frac{\dot{\delta}}{\lambda} \right) \tag{9}$$

where the quantity  $(\Delta \dot{P}/\lambda)$ , called *Doppler shift offset* [Garriott and Bracewell, 1961], is the difference between the Doppler shift observed and the Doppler shift that would have been observed in the absence of the ionosphere. Figure 2 displays the Doppler shift offset and the Doppler shift curves as functions of time for a passage of the satellite Transit 2-A.

If the satellite is above most of the ionization, the principal contribution to  $P$  will occur near the height ( $h_{max}$ ) of the maximum electron density, and since the geometrical factor  $\sec \chi$  (Fig. 3) is a slowly varying function, we can write, from (4),

$$\begin{aligned} \Delta P &= \frac{K_1}{2f^2} \int_0^{h_s} N \sec \chi dh \\ &\approx \frac{K_1}{2f^2} \sec \chi_m \int_0^{h_s} N dh \end{aligned} \tag{10a}$$

or

$$\Delta P \approx \frac{K_1}{2f^2} \sec \chi_m I \tag{10b}$$

The quantity

$$I = \int_0^{h_s} N dh$$

is called the *columnar density* and is equivalent to the total number of electrons in a column of unit base, extending from the ground to the height of the satellite,  $h_s$ .

Differentiating (10b) with respect to time and dividing the result by the free-space wavelength of the fundamental frequency, we obtain a differential equation relating to Doppler shift offset  $\Delta \dot{P}/\lambda$  given by (9) with the columnar density  $I$ :

$$\left( \frac{\Delta \dot{P}}{\lambda} \right) = \frac{K_1}{2f^2 \lambda} \left[ I \frac{d}{dt} (\sec \chi_m) + \sec \chi_m \dot{I} \right] \tag{11}$$

or

$$\begin{aligned} \dot{I} - \left[ \sec \chi_m \frac{d}{dt} (\cos \chi_m) \right] I \\ = 2f^2 \lambda K_1^{-1} \cos \chi_m \left( \frac{\Delta \dot{P}}{\lambda} \right) \end{aligned} \tag{12}$$

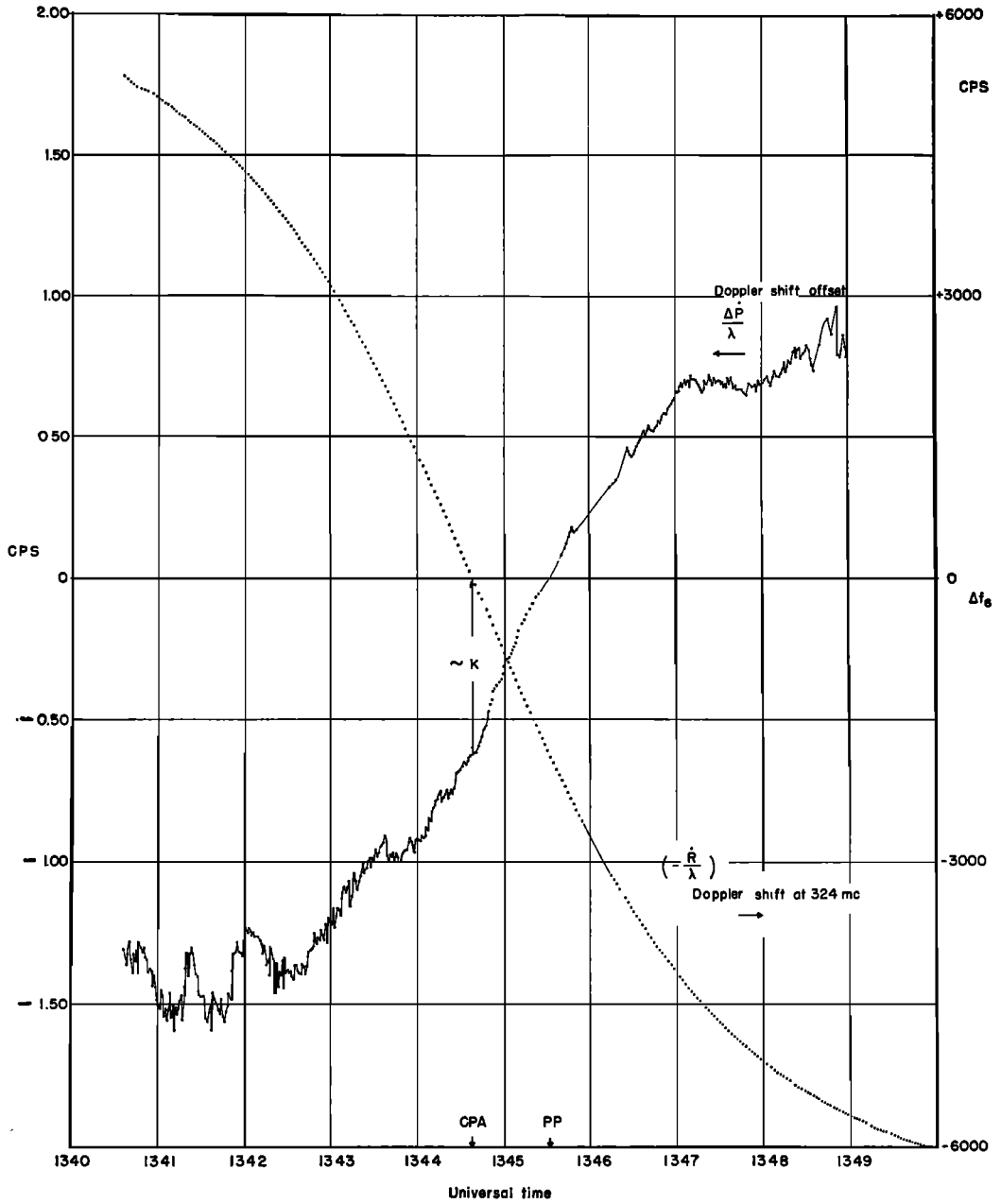


Fig. 2. Morning passage of satellite Transit 2-A on July 29, 1960, while close to apogee ( $\dot{h} = -20$  m/sec), showing Doppler shift offset when irregularities in electron distribution are weak. Doppler shift of the 324-Mc/s channel is also shown.

or

$$\dot{I} + f_1(t)I = f_2(t) \quad (13)$$

The problem is now reduced to solving the first-order and linear differential equation 13

for  $I(t)$  where the functions  $f_1(t)$  and  $f_2(t)$  are known functions of time. For this we need one boundary, namely the value of  $I$  at any time  $t$ , but our observational data do not provide us with this quantity directly. This boundary can

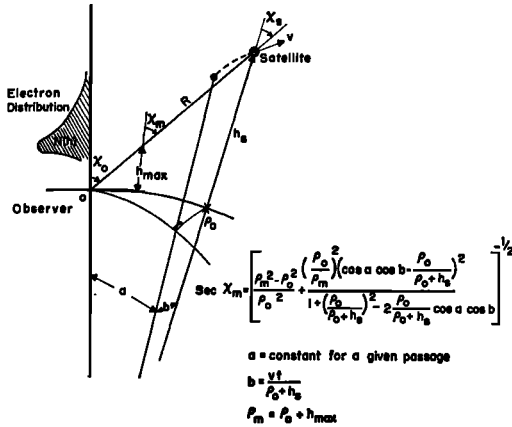


Fig. 3. Geometry of the problem for calculation of  $\chi_m(h_s, h_m, v, t)$ .

be found from a combination of the Doppler data and the Faraday rotation-angle information [de Mendonça and Garriott, 1962a], but for the moment we will use another approach. From (10),

$$I = 2f^2 K_1^{-1} \cos \chi_m \Delta P = F(t) \Delta P \quad (14)$$

where  $F(t) = 2f^2 K_1^{-1} \cos \chi_m$  is a known factor. We can integrate the Doppler shift offset measurement and obtain

$$\Delta P = \Delta P_0 + \lambda \int \left( \frac{\Delta \dot{P}}{\lambda} \right) dt \equiv \Delta P_0 + \Delta P_i \quad (15)$$

The operation of integration is equivalent to a low-pass filtering process; thus, even though the differential Doppler might be quite irregular, the resulting curve obtained for  $\Delta P_i$  is usually smooth, as shown by the curve in Figure 4. We can rewrite (14) as

$$I(t) = F(t)(\Delta P_0 + \Delta P_i) \quad (16)$$

and we are justified in expecting  $I(t)$  to be a relatively smooth curve. Note that  $\Delta P_i$  as defined by (15) can be obtained also by merely counting the cycles of the differential Doppler beat and multiplying the results by  $n^2(n^2 - 1)^{-1}\lambda$ .

From the geometry of the system, we know that there is a time  $t = t_c$  such that

$$(d/dt)(\cos \chi_m)_{t=t_c} = 0 \quad (17)$$

Then, from (12) and the above considerations, we may assume to a good approximation that,

in the neighborhood of  $t_c$ , we have an average value for the slope of  $I(t)$  given by

$$K = \dot{I}]_{t=t_c} = f_2(t_c) = 2f^2 \lambda K_1^{-1} \cos \chi_m(t_c) \left[ \frac{\Delta \dot{P}}{\lambda} \right]_{t=t_c} \quad (18)$$

where  $\overline{(\Delta \dot{P}/\lambda)}_{t=t_c}$  is a smoothed value of the Doppler shift offset at time  $t_c$ , which can be obtained as shown in the curve of Figure 2. Also, using (11) and (16) for an interval centered at  $t_c$ , we can define the function  $A(t)$  as the first approximation to the Doppler shift offset:

$$A(t) = \frac{K_1}{2f^2 \lambda} \left[ F(t)(\Delta P_0 + \Delta P_i) \frac{d}{dt} \cdot (\sec \chi_m) + K \sec \chi_m \right] \quad (19)$$

$$= \frac{\cos \chi_m(t_c)}{\cos \chi_m(t)} \left( \frac{\Delta \dot{P}}{\lambda} \right)_{t_c} - \frac{\Delta P_0 + \Delta P_i}{\lambda \cos \chi_m(t)} \frac{d}{dt} (\cos \chi_m) \quad (20)$$

All the quantities involved in  $A(t)$  are known with the exception of  $\Delta P_0$ . Since the Doppler shift offset  $\Delta \dot{P}/\lambda$  is measured at the discrete times  $t_i = (t - t_{P\Delta}) = 0, \pm 1, \pm 2, \dots, \pm 250$  sec, we can write

$$S_c = \sum_i [A_i - (\Delta \dot{P}_i/\lambda)]^2 \quad (21)$$

and minimize  $S_c$  by varying the value of  $\Delta P_0$ . The value of  $\Delta P_0$  that minimizes the sum indicated by (21) establishes the necessary boundary condition to the differential equation 13.

This minimization can be done in a digital computer. The initial objective is to determine the constant of integration  $\Delta P_0 = C_0$  and a posteriori use it in (16) for determining  $I(t)$ . As a starting point we need a first estimate of  $C_0$ . This estimation can be included in the computer program if we reason as follows. The electron content  $I(t)$ , given by (16), is the product of two functions of time: one,  $\cos \chi_m(t)$ , has maximum at  $t = t_c$  and is concave downward; the other,  $\Delta P$ , has a minimum at  $t = t_{PF}$  and is concave upward. Thus,  $I(t)$  will tend to be concave upward or downward, depending on whether  $C_0$  is under or overestimated. This reasoning leads us to assume that, if  $C_0$  is properly estimated, the resultant  $I(t)$

29 JULY 1960, Transit 2 A  
pass # 529

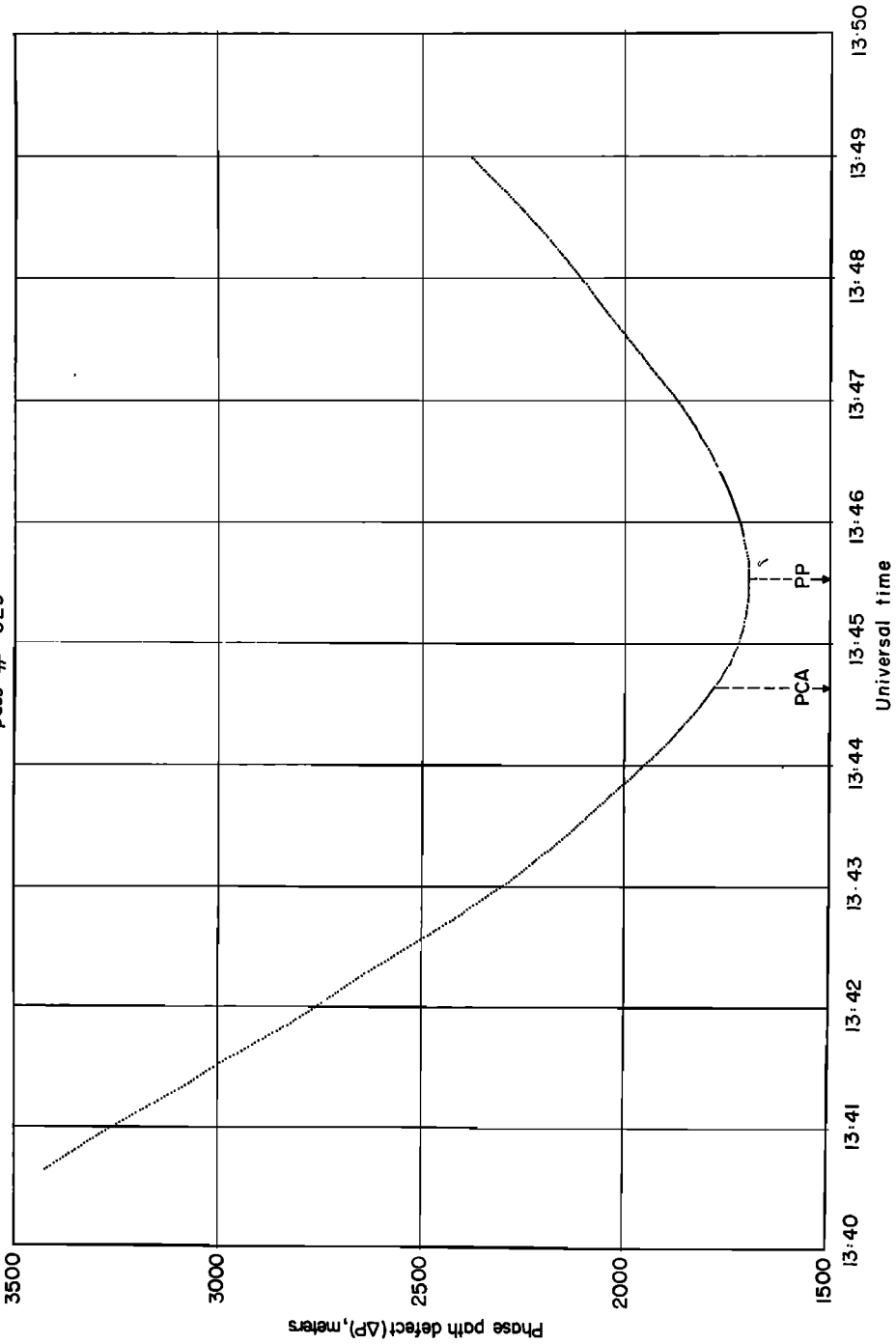


Fig. 4. Phase path defect ( $\Delta P = \Delta P_t + \Delta P_o$ ). The quantity  $\Delta P_t$  is obtained by numerical integration of the Doppler shift offset measurement (Fig. 2) and  $\Delta P_o$  is a computed constant of integration. Note the asymmetry with respect to the point of closest approach (PCA) caused by horizontal gradients.

within a reasonable interval would be linear with time; that is, it would be of the form

$$I(t) \approx Kt + B \quad (22)$$

or

$$I(t) \approx \frac{F_i(\Delta P_i + C_0) - F_0 C_0}{t_i} t + F_0 C_0 \quad (23)$$

where  $F_i = F(t) = 2f^2 K_1^{-1} \cos \chi_m$ . The slope of  $I(t)$  given above can be represented by the value of  $K$  already defined by (18);

$$K = [F_i(\Delta P_i + C_0) - F_0 C_0]/t_i \quad (24)$$

or

$$C_0 = (Kt_i - F_i \Delta P_i)/(F_i - F_0) \quad (25)$$

Instead of obtaining  $C_0$  from only one point of (25), we can use several points and establish an average  $C$ , defined as

$$C = \frac{1}{|m| + |n| + 1} \sum_{i=-m}^{i=n} \frac{Kt_i - F_i \Delta P_i}{F_i - F_0} \approx \Delta P_0 \quad (26)$$

The value of  $C$ , given by this equation, is our first estimation of  $\Delta P_0$  and is to be used as an initial step in the minimization of the sum of squares defined by (21).

Once the final value of  $\Delta P_0$  is obtained by means of a polynomial best-fit approximation, (16) is used to provide the output  $I(t)$  in listing and cards, which were used on an X-Y plotter, resulting in graphs, like the one shown in Figure 5.

Note that the assumption of smoothness of  $I(t)$  for considerable intervals of time is satisfied for this passage.

#### DISCUSSION OF THE APPROXIMATIONS

*High-frequency approximation.* The complete Appleton-Hartree equation for the refractive index of a medium containing free electrons, with a superimposed steady magnetic field, is given in the usual notation [Ratcliffe, 1959] by

$$\begin{aligned} n^2 &= (\mu - ick/\omega)^2 \\ &= 1 - X\{1 - iZ \\ &\quad - (1/2) [Y_T^2/(1 - X - iZ)] \\ &\quad \pm \sqrt{[\frac{1}{2} Y_T^2/(1 - X - iZ)]^2 + Y_L^2}\}^{-1} \end{aligned} \quad (27)$$

In the most unfavorable cases of the experiment, we are considering the following values of  $X$ ,  $Y$ , and  $Z$  at  $F$ -layer heights and at a wave frequency of 54 Mc/s:

$$X_0 = (f_0 F_2/f)^2 < 0.07 \quad (28)$$

$$Y = f_H/f \approx 0.02 \quad (29)$$

$$Z = \nu/\omega < 10^{-5} \quad (30)$$

Thus, the quasi-longitudinal approximation condition [Ratcliffe, 1959] given by the inequality

$$Y_L^2 \gg Y_T^4/4 |1 - X - iZ|^2 \quad (31)$$

reduces to

$$\cos \theta > \frac{1}{2} Y \sin^2 \theta \quad (32)$$

or

$$\theta < 89^\circ \quad (33)$$

The magnetic-dip angle at Stanford is approximately  $62^\circ$ , and it may be shown that the inequality 33 is satisfied for zenith angles up to  $75^\circ$  in any azimuth from Stanford. On the basis of these considerations we can rewrite (27) to a very good approximation:

$$\mu^2 \approx 1 - K_1 N/f(f \pm f_H \cos \theta) \quad (34)$$

$$\begin{aligned} \mu^2 &\approx 1 - K_1 N(1 \mp 0.02 \cos \theta)/f^2 \\ &\approx 1 - (K_1 N/f^2) \end{aligned} \quad (35)$$

The error in  $\mu^2$ , using (35) instead of (27), is much less than 1 per cent. As was mentioned before, in the most unfavorable circumstances of the experiment, the value of  $X_0 = K_1 N/f^2$  was smaller than 0.07, and in the majority of cases it was smaller than 0.04. Thus, the binomial expression for  $\mu$ , which is

$$\begin{aligned} \mu &\approx 1 - (\frac{1}{2})(K_1 N/f^2) - (\frac{1}{8})(K_1 N/f^2)^2 \\ &\quad - (\frac{1}{16})(K_1 N/f^2)^3 - \dots \end{aligned} \quad (36)$$

can be represented to a good approximation by (1), namely,

$$\mu \approx 1 - K_1 N/2f^2 \quad (37)$$

*Refraction approximation.* In deriving (5) it was implicitly assumed that refraction effects could be neglected. It can be shown that, in the case of a flat ionosphere approximation, we have

$$\begin{aligned} D &\equiv R - \int_0^s ds \\ &\leq (R/32)\chi^2 \tan^2 \chi_0 \propto 1/f^4 \end{aligned} \quad (38)$$

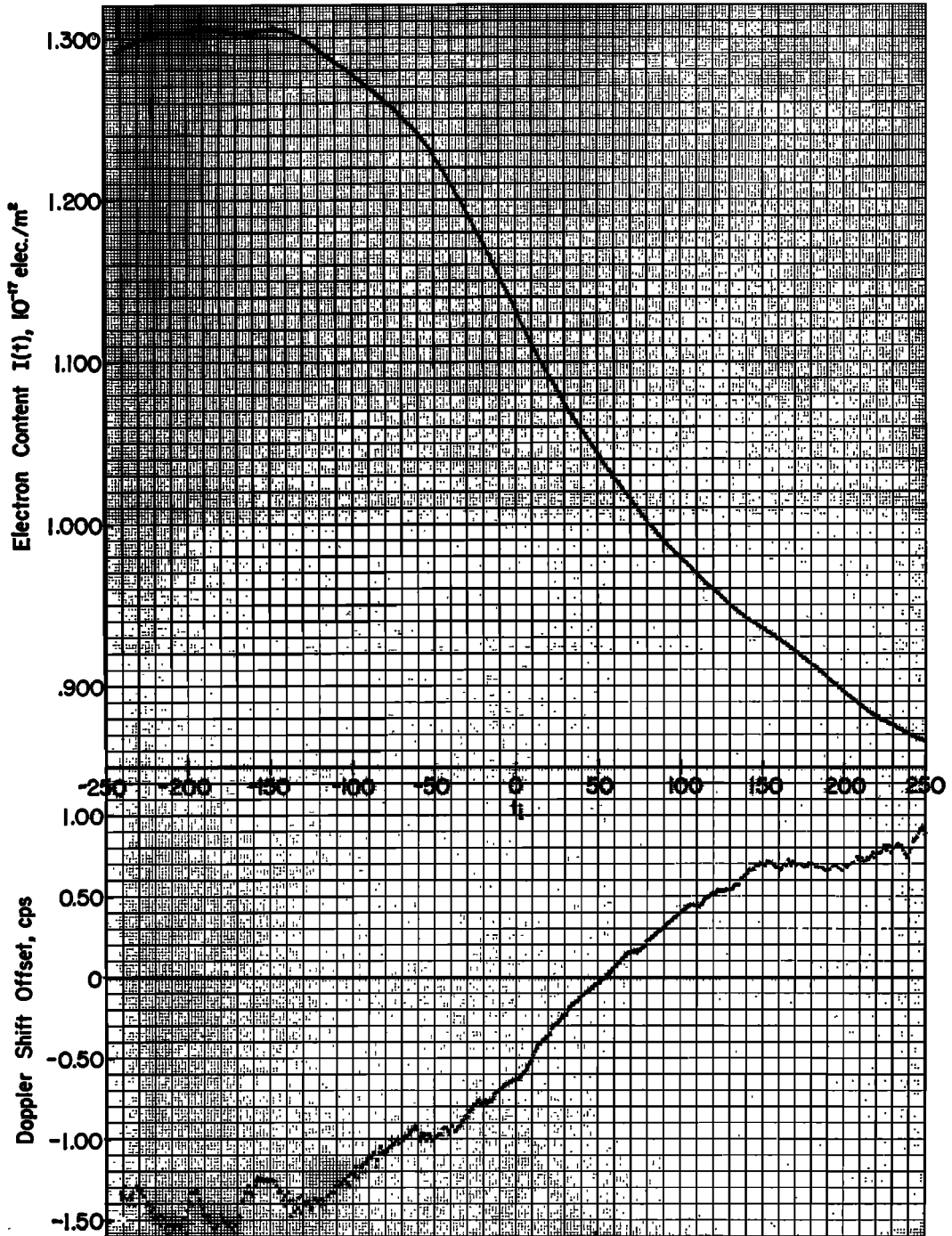


Fig. 5. Calculated electron content  $I(t)$  and measured differential Doppler frequency as a function of time ( $t$ , in seconds) for a northbound passage of the satellite Transit 2-A with PCA at 05h 44m 38s LMT,  $h_s = 1053$  km,  $\dot{h}_s = -22$  m/sec, on July 29, 1960.

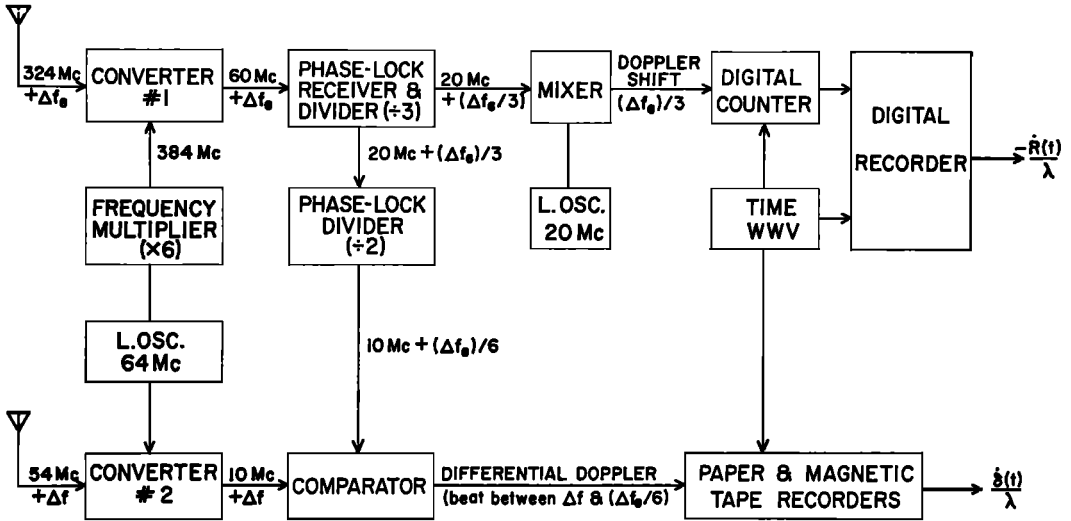


Fig. 6. Diagram of system used for measurement of Doppler shift and differential Doppler in transmissions of satellite 1960η₁.

Thus, at the frequencies used, the 'straight-line approximation,' which is equivalent to  $D = 0$ , contributes an error of less than 1 per cent in the evaluation of the phase path defect  $\Delta P$  when the zenith angle is  $60^\circ$ . For zenith angles smaller than  $40^\circ$  the error introduced by this approximation is practically zero. Since the value of  $R$  cannot be greater than

$$\int_0^s ds$$

the error is toward an overestimation of the columnar density

$$I = \int_0^{h^*} N dh$$

for very large zenith angle  $\chi$ . This situation was taken into consideration in the analysis of the data by limiting the time of the observation to a maximum of 300 sec from the point of closest approach of the satellite and primarily using passages with  $\chi_{\min}$  smaller than  $45^\circ$ .

It will be seen in the final results that, in the plots representing  $I(t)$ , there is no consistent tendency toward higher values of columnar density at the beginnings and ends of the curves.

**Magnetic-field effects.** Under the conditions of the experiment—an observer in the northern hemisphere receiving a left-hand, elliptically polarized wave with an antenna of the same

polarization—the differential Doppler measurement will result in the measurement of the phase path defect of the ordinary mode as shown by *de Mendonça and Garriott* [1962b].

Combining (4) and (34), we can write the phase path defects of the ordinary and extraordinary waves:

$$\begin{aligned} \Delta P_{o,z} &= \int_0^s (1 - \mu) ds \\ &\approx \Delta P(1 \mp Y \cos \theta) \end{aligned} \quad (39)$$

then

$$\Delta P_o \leq \Delta P \leq \Delta P_z \quad (40)$$

where  $\Delta P$  would be the phase path defect in the absence of the magnetic field of the earth. Equation 39 implies that, in the present problem, without corrections, the calculated value of  $I(t)$  derived from differential Doppler measurements will be underestimated by a factor of the order of the anisotropy in  $(1 - \mu)$ , that is, less than 2 per cent.

The errors introduced by the refraction approximation and by the presence of the magnetic field of the earth are of the same magnitude but with opposite signs. That is, the former is toward an overestimation, the latter, an underestimation, of the value of  $I(t)$ . As a consequence, it has been decided to present the

TABLE 1. Northbound Passages of the Satellite 1960 $\eta_1$  during Sunrise Hours  
 For this group of passages the apogee was very close to PCA, thus,  $t_c \approx t_T \approx t_0$ .

Date, 1960	Revolution Number	$\dot{h}_s(0)$ , m/sec	$h_s(0)$ , km	$x_{\min}$ , deg	$t_0$ PCA, LMT, 120°W	$t_c - t_0$ , sec	$t_T - t_0$ , sec
July 23	0445	-10	1064	19	07h 25m 32s		
July 24	0459	-12	1064	21	07 08 44		
July 25	0473	-16	1064	24	06 51 55		
July 26	0487	-18	1064	27	06 35 06		
July 27	0501	-20	1063	29	06 18 17		
July 28	0515	-21	1063	31	06 01 32		
July 29	0529	-22	1063	33	05 44 38		
July 30	0543	-23	1062	36	05 27 52		
July 31	0557	-25	1062	38	05 11 03		
Aug. 1	0571	-27	1062	40	04 54 16		
Aug. 2	0585	-29	1061	42	04 37 26		
Aug. 3	0599	-32	1061	44	04 20 37		
Aug. 4	0613	-34	1061	46	04 03 48		
Aug. 5	0627	-38	1060	48	03 46 57		
Aug. 6	0641	-39	1060	49	03 30 04		
Aug. 7	0655	-40	1060	51	03 13 19		
Aug. 8	0669	-42	1059	52	02 56 34		

approximately zero

approximately zero

TABLE 2. Northbound Passages of the Satellite 1960 $\eta_1$  during the Afternoon and Sunset Hours

Note that the apogee is not too far from PCA and that the satellite is above most of the ionosphere.

Date, 1960	Revolution Number	$\dot{h}_s(0)$ , m/sec	$h_s(0)$ , km	$x_{\min}$ , deg	$t_0$ PCA, LMT, 120°W	$t_c - t_0$ , sec	$t_T - t_0$ , sec
Sep. 6	1090	-128	1020	43	20h 15m 08s	-5.5	-2.9
Sep. 7	1104	-129	1019	45	19 58 14	-5.8	-3.2
Sep. 8	1118	-129	1018	47	19 41 21	-6.2	-3.4
Sep. 9	1132	-130	1017	50	19 24 29	-6.4	-3.4
Sep. 14	1203	-163	984	43	19 44 27	-7.0	-3.7
Sep. 15	1217	-160	982	41	19 27 30	-7.0	-3.8
Sep. 17	1245	-164	981	37	18 53 43	-7.0	-4.0
Sep. 18	1259	-164	978	35	18 36 49	-6.5	-4.1
Sep. 19	1273	-165	977	32	18 19 53	-6.0	-4.2
Sep. 20	1287	-171	975	29	18 02 58	-5.4	-4.2
Sep. 21	1301	-173	975	27	17 46 02	-5.0	-4.1
Sep. 26	1371	-175	967	11	16 21 32	-4.2	-4.0
Sep. 27	1385	-175	966	7	16 04 36	-4.1	-4.0
Sep. 28	1399	-176	964	3	15 47 44	-4.0	-4.0
Oct. 2	1455	-181	960	10	14 40 05	-5.0	-4.1
Oct. 3	1469	-183	959	14	14 23 11	-5.0	-4.1
Oct. 4	1483	-185	957	17	14 06 20	-5.0	-4.1
Oct. 5	1497	-187	953	21	13 49 23	-5.5	-4.2
Oct. 6	1501	-189	951	24	13 32 33	-6.0	-4.5
Oct. 7	1515	-189	950	27	13 15 38	-6.5	-5.0
Oct. 10	1557	-189	943	35	12 24 57	-7.0	-5.1
Oct. 11	1571	-189	943	38	12 08 00	-8.0	-5.1
Oct. 13	1599	-192	941	43	11 34 11	-9.0	-5.1

TABLE 3. Southbound Passages of the Satellite 1960 $\eta_1$

Date, 1960	Revolution Number	$h_p(0)$ , m/sec	$h_s(0)$ , km	$\chi_{min}$ , deg	$t_0$ PCA, LMT, 120°W	$t_c - t_0$ , sec	$t_T - t_0$ , sec
Aug. 1	0577	-222	743	48	15h 34m 17s	-8.3	-3.3
Aug. 2	0591	-222	741	46	15 17 28	-7.6	-3.3
Aug. 3	0605	-222	741	43	15 00 36	-6.3	-3.3
Aug. 4	0619	-222	739	41	14 43 46	-5.6	-3.3
Aug. 6	0647	-222	737	35	14 10 05	-5.1	-3.4
Aug. 7	0661	-223	734	32	13 53 16	-4.9	-3.5
Aug. 8	0675	-223	731	28	13 36 26	-4.7	-3.6
Aug. 9	0689	-223	730	24	13 19 36	-4.4	-3.6
Aug. 10	0703	-223	729	20	13 02 45	-4.2	-3.7
Aug. 11	0717	-220	728	16	12 45 51	-4.1	-3.8
Aug. 12	0731	-217	727	12	12 29 02	-3.9	-3.8
Aug. 13	0745	-215	726	7	12 12 12	-3.9	-3.9
Aug. 14	0759	-213	724	3	11 55 21	-3.9	-3.9
Aug. 15	0773	-211	723	2	11 38 29	-3.9	-3.9
Aug. 16	0787	-210	722	7	11 21 36	-3.9	-3.9
Aug. 19	0829	-207	716	19	10 31 06	-4.2	-3.7
Aug. 21	0857	-205	712	26	09 57 26	-4.7	-3.6
Aug. 23	0885	-203	710	32	09 23 29	-4.9	-3.5
Aug. 25	0913	-202	709	38	08 49 41	-5.4	-3.4
Aug. 26	0927	-200	707	41	08 32 50	-5.8	-3.3
Aug. 27	0941	-198	706	43	08 15 58	-5.9	-3.2
Aug. 28	0955	-196	705	46	07 59 02	-6.6	-3.1
Aug. 29	0969	-194	704	48	07 42 09	-7.0	-3.1
Aug. 30	0983	-192	703	50	07 25 15	-7.0	-3.0
Sep. 14	1194	-150	660	30	04 56 04	-2.7	-1.7
Sep. 15	1208	-149	660	27	04 39 11	-2.4	-1.8
Sep. 16	1222	-148	660	22	04 22 16	-2.2	-1.8
Sep. 19	1264	-146	658	9	03 31 32	-2.0	-2.0

calculations of  $I(t)$  without a variable correction for this combination of errors.

EXPERIMENTAL PROCEDURE

Differential Doppler measurements were made using about 70 passages of the satellite 1960 $\eta_1$  with the system schematically shown in Figure 6. The outputs of this system have already been displayed in Figures 1 and 2.

The sampling for the differential Doppler measurement was done (using paper-tape recordings) by measuring the beat frequency ( $\delta/\lambda$ ) at every second of the passage of the satellite. Near the proximal point (PP), or whenever the beat frequency was less than  $1/2$  cps, the sampling interval had to be lengthened to correspond to half a cycle of the beat. The precision in measuring time intervals was of the order of 20 msec. For intervals in which the phase-lock receiver showed periods of 'unlocked signal,' we made interpolations. The purpose of the interpolations in  $\delta/\lambda$  was to simplify the computer program for the computation of  $\int N dh$ . Later, the inter-

polated points were removed before the results reached the plotting machine, so that the plots would show only the actually measured values of Doppler shift offset.

Data of the satellite passages under consideration in this paper, with some of the orbital parameters, are presented in Tables 1, 2, and 3. In these tables, the first five columns were obtained from the ephemerides for the satellite. The last three columns were obtained by combining elements of the ephemerides with the measured values of Doppler shift  $-\dot{R}/\lambda$ , with consideration of the reasoning that follows.

In the vicinity of  $t = t_0$ , it is permissible to use the flat-earth approximation for the range  $R$ :

$$R \approx h_s \sec \chi \tag{41}$$

Differentiating (41) with respect to time we obtain

$$\dot{R}(t) \approx \dot{h}_s(t) \sec \chi + h_s(t)(d/dt)(\sec \chi) \tag{42}$$

Then, since at  $t = t_0$  the value of  $\chi$  is a minimum,

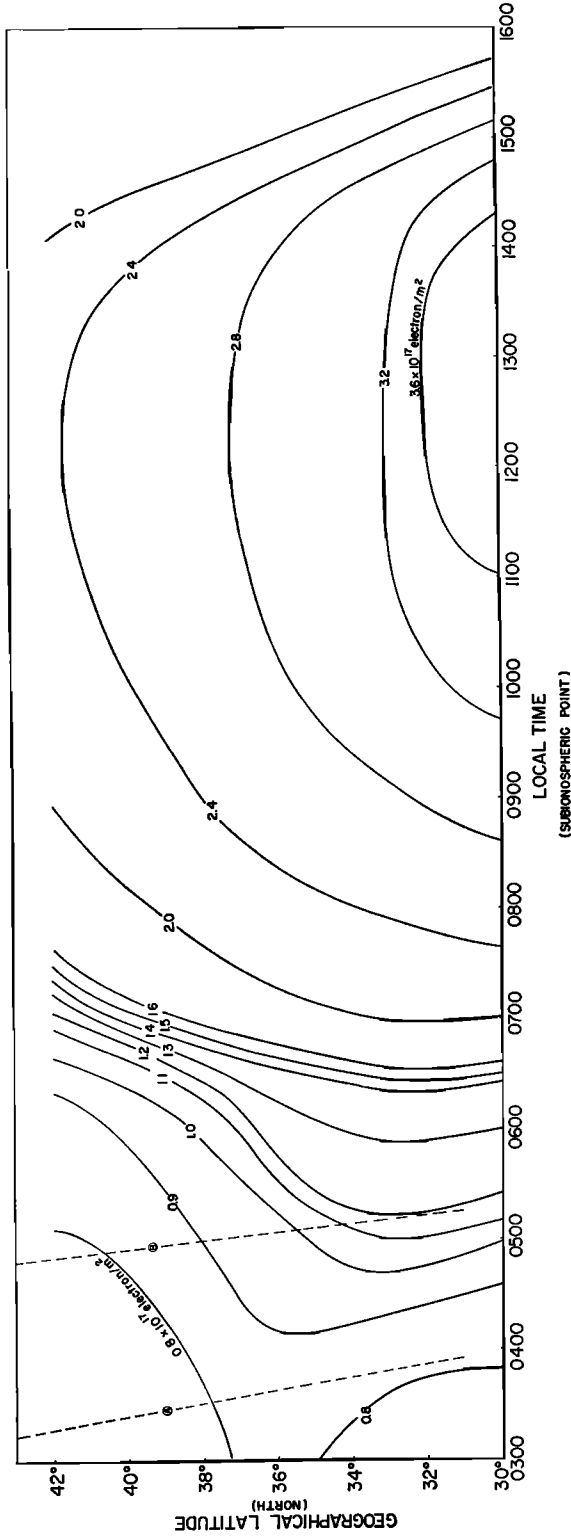


Fig. 7. Smoothed curves of constant  $\int N dh$  derived from measurements on quiet days during July and August 1960 (Tables 1 and 3). Curve 4 represents sunrise at sea level and curve B sunrise at height  $h = 400$  km for July 29, 1960.

and

$$[(d/dt) \sec \chi]_{t-t_0} = 0 \tag{43}$$

we can write

$$\dot{R}(t_0) \approx \dot{h}_s(t_0) \sec \chi_{\min} \tag{44}$$

From the ephemerides, and the Doppler shift measurements, it can be seen that in the interval  $|t_i| < 20$  sec the values of  $\dot{h}_s$  and  $\dot{R}$  are almost constant.

Then

$$\ddot{R}(t_0) \approx \ddot{R}(t_0) \approx \ddot{R}(t_T) \tag{45}$$

and

$$\dot{h}_s(t_0) \approx \dot{h}_s(t_0) \approx \dot{h}_s(t_T) \tag{46}$$

where  $t_T$  is the time at which the plane of the orbit and the vertical plane (through observer, satellite, and center of the earth) are at right angles. Note that the position of this transverse time  $t_T$  can be determined by the base of the perpendicular from the observer to the sub-satellite track. Since, at the PCA,  $t_i = 0$  and  $\dot{R}(t_0) = 0$ , (44), (45), and (46) can be combined to give a simplified expression for the Doppler shift at time  $t_0$ :

$$-\dot{R}(t_0)/\lambda \approx -[\dot{h}_s(t_0)/\lambda] \sec \chi_{\min} \tag{47}$$

Since the second member of (47) is a known quantity, we can easily determine the value of  $t_0$  from the measured Doppler shift curve. Similarly, with the same considerations described above, we can also determine the value of  $t_T$  from the approximate expression:

$$-\dot{R}(t_T)/\lambda \approx -[\dot{h}_s(t_0)/\lambda] \cos \chi_{\min} \tag{48}$$

For the satellite passages considered in this paper, the vertical velocity  $\dot{h}_s(t)$  was never positive. Then, when not in coincidence, the three points above would take place in the order  $t_0$ ,  $t_T$ , and  $t_i$  respectively.

The output of the system, shown in Figure 6, and the necessary orbital elements were used as the input for the calculations of the columnar electron density  $\int N dh$ . These calculations were performed with a Burroughs 220 digital computer at the Stanford Computational Center.

The input, described here as Doppler shift offset, obtained from differential Doppler through (9), and the output  $\int N dh$  were plotted by machine as shown in Figure 5.

Note that, even though the absolute value of

$I(t)$  might be in error by a few per cent as a result of errors in the computation of  $\Delta P_0$ , the relative values of  $I(t)$ , within a given curve, are very accurate and may be represented with four digits as shown on the plot of  $I(t)$ .

#### ANALYSIS AND RESULTS

*Horizontal gradients in  $I(t)$  during magnetically quiet days.* The intersection of the ray with a shell at the height  $h_{\max}$  of the maximum electron density is called the *ionospheric point*, and the projection of this point on the ground is the *subionospheric point*. When  $I(t)$  is combined with the information about the position of the satellite, as a function of time, obtained from the ephemerides, we can determine the electron content as a function of the local time (LT) and latitude of the subionospheric point. This was done for the passages listed in Tables 1, 2, and 3, occurring on nondisturbed days. Lines of constant values of  $\int N dh$  were smoothed through the points thus obtained, and the resultant curves are presented in Figures 7 and 8.

Sunrise lines at sea level and at the height of 400 km are shown by curves *A* and *B* in Figure 7. Similarly, the sunset lines are indicated in Figure 8. It should be noted that for the region under consideration the horizontal gradients of the electron distribution are essentially along the meridians during the early afternoon, becoming east-west at sunrise and sunset. The south-north gradient results in a decrease of about 25 per cent in  $\int N dh$  for two subionospheric points separated by a distance of 1000 km; the west-east value at the latitude 35°N at sunset (close to equinox) was observed to cause about the same decrease in  $\int N dh$  for the same distance of 1000 km. It must be remembered that we are considering a region with geographic latitudes in the range of approximately 30°N to 45°N (or geomagnetic 37°N to 51°N). It is not implied that horizontal gradients with such magnitudes can exist at all latitudes.

In general the value of  $I(t)$  may vary as a result of horizontal gradients and variations in the height  $h_s$  of the satellite; however, for all the passages considered in this paper, the satellite was above 650 km with  $|\dot{h}_s| < 230$  m/s; thus, the effect of the variation in  $h_s$  on  $I(t)$  was very small. The southbound passages observed displayed an increase in  $I(t)$  as in Figure 9 even though the satellite had a decreasing height.

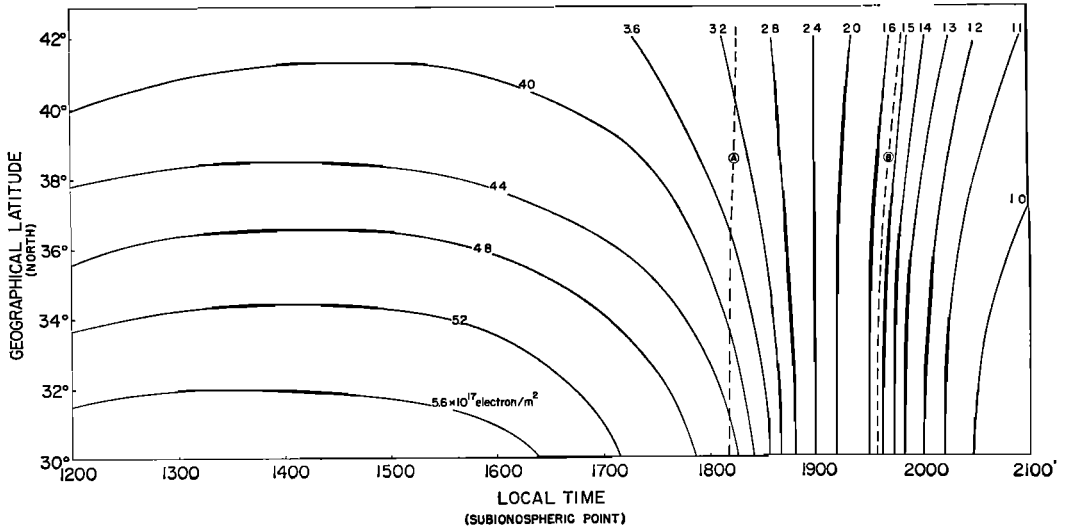


Fig. 8. Smoothed curves of constant  $\int N dh$  derived from measurements on quiet days during September and October 1960 (Table 2). Curve A represents sunset at sea level and curve B sunset at height  $h = 400$  km for September 12, 1960.

Note, also, that in comparing the results shown in Figures 7 and 8 there is a difference in the values of  $\int N dh$  for the same latitudes between 1200 and 1600 (local time). This difference is probably caused by a seasonal effect that can best be seen in Figure 10, where  $\int N dh$  is plotted as a function of local time of the subionospheric point and has the latitude as a parameter.

*Magnetic storm effects on  $I(t)$ .* Unfortunately, the period of observations did not extend long enough to permit making a more detailed or statistical study of the effects of magnetic storms on the total electron content. However, the two storms of August 16 and October 6, 1960, were observed. The latter was particularly strong and reached values of  $\Sigma K_p = 63$  out of a maximum of  $\Sigma K_p = 72$  for a period of 24 hours.

Since for the dates considered the satellite passages were around midday, the horizontal gradients involved were essentially in the north-south direction. The August storm caused a considerable increase in the horizontal gradients of the distribution, as can be seen in Figure 11, which also shows that the disturbance resulted in an increased  $I(t)$  as compared with the average quiet-day value (positive disturbance) for geographic latitudes smaller than  $39^\circ N$ . Figure 12 shows the observed effects for the

stronger storm (October) which was primarily a negative disturbance along the range of latitudes surveyed. The day with the intermediate value of  $A_p = 36$  produced the largest horizontal gradients, causing a decrease of about 50 per cent in  $\int N dh$  for a latitudinal variation of the subionospheric point of approximately  $7^\circ$ .

Note that on the date when the magnetic index was a maximum,  $A_p = 206$  on October 6, 1960, and the early afternoon values of  $\int N dh$  reached an over-all minima of the order of values encountered during normal nights.

Combining the value of  $I(t)$  at the point of closest approach, that is  $I(0)$ , and the critical frequency  $f_oF_2$  obtained about the same time at Stanford, we can establish the equivalent column height  $I(0)/N_{\max}$ . This quantity was calculated for all the passages of the satellite for which a corresponding Stanford ionogram had been obtained, and the results are plotted in Figure 13, where  $I(0)/N_{\max}$  appears versus the geomagnetic index  $A_p$ . The general tendency is toward higher equivalent column heights for increasing values of  $A_p$ , beyond a threshold of  $A_p \approx 30$ . This tendency was particularly noticeable during the two storms mentioned above and implies that the decrease in  $N_{\max}$  is accompanied by an increase in the layer thickness.

These results seem to be consistent with those

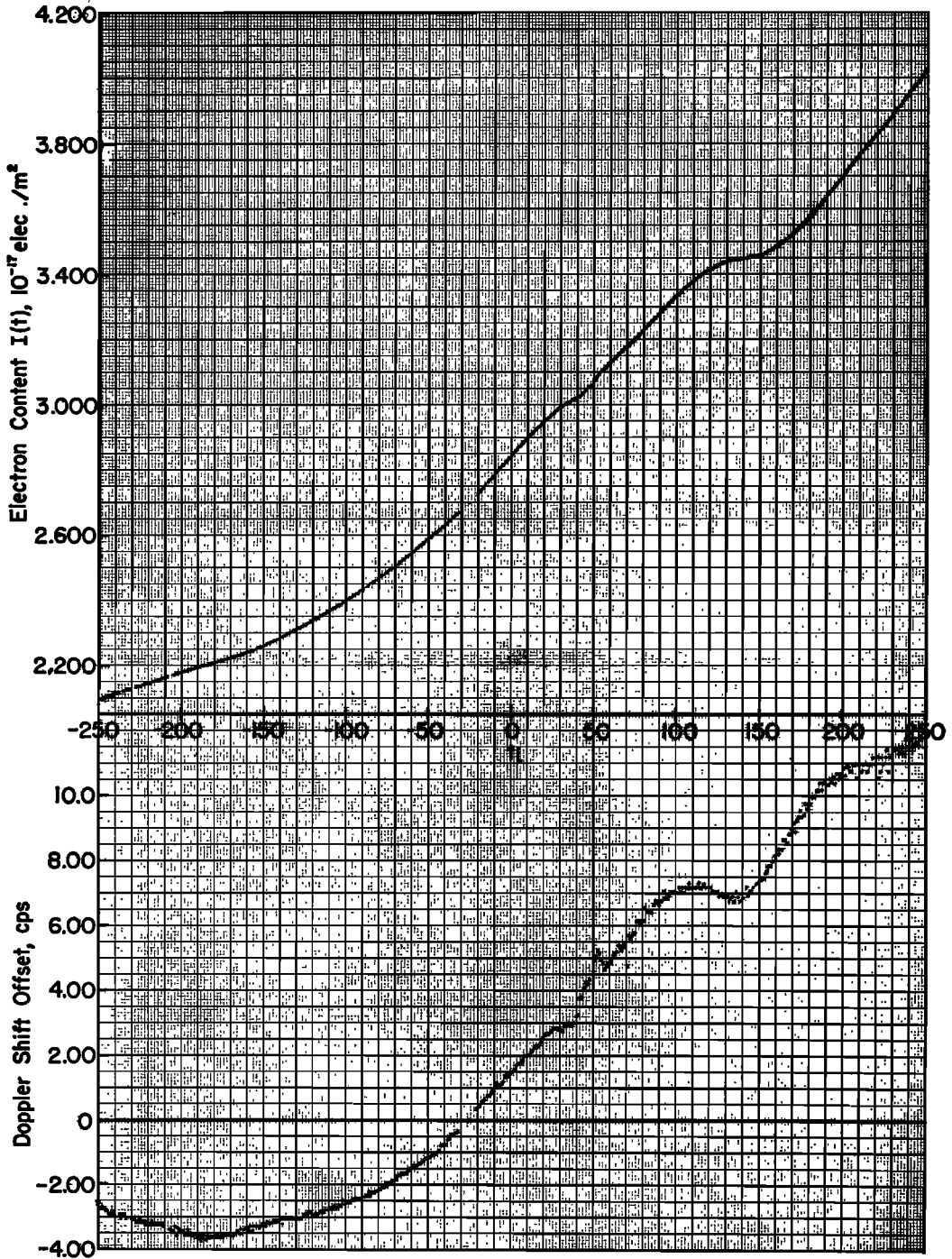


Fig. 9. Electron content and Doppler shift offset as a function of time ( $t$ , in seconds) for a southbound passage of the satellite Transit 2-A with PCA at 13h 02m 45s (LMT) and  $\dot{h}_s = -223$  m/sec on August 10, 1960.

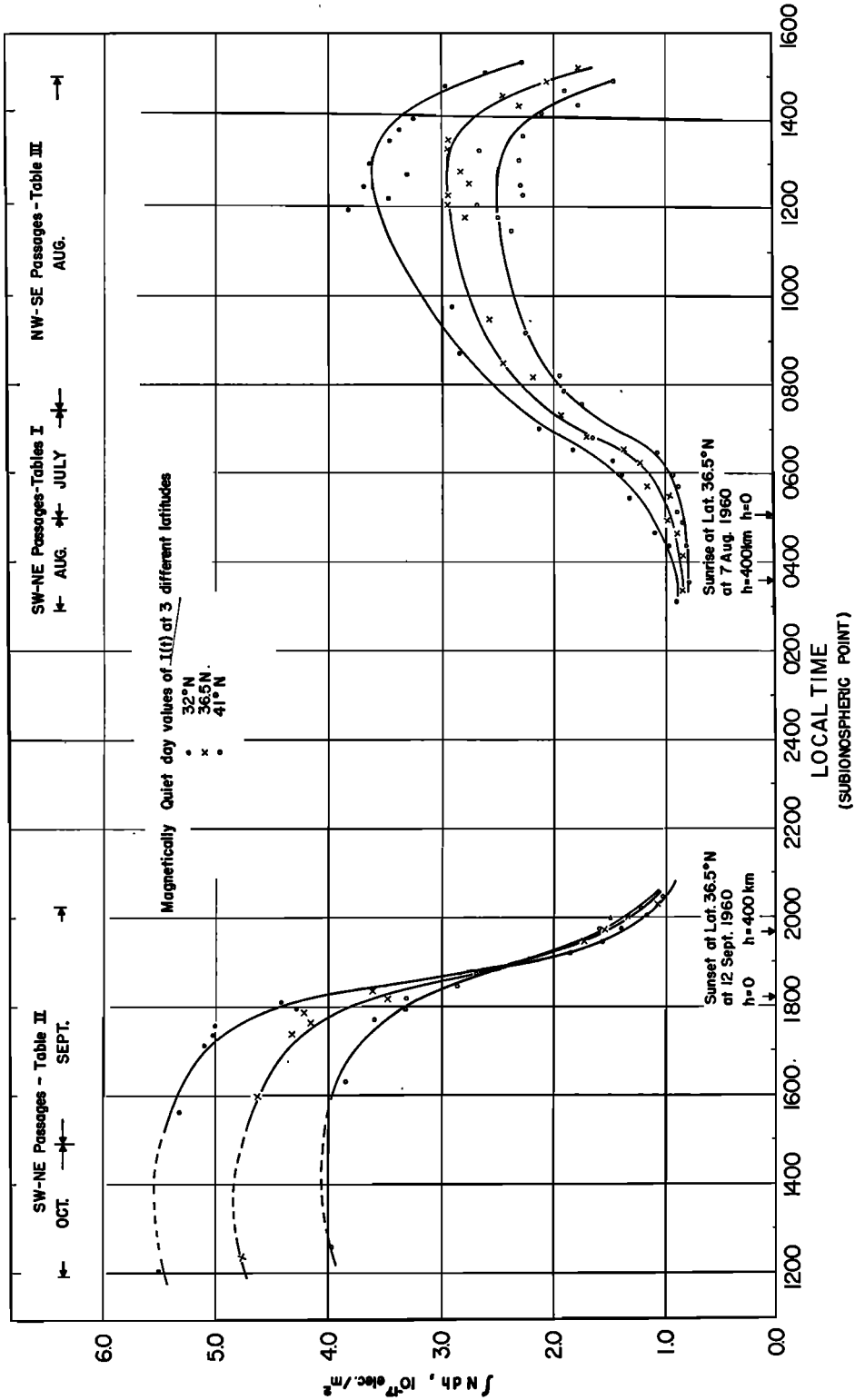


Fig. 10. Quiet-day values of  $\int N dh$  as a function of local time of subionospheric point averaged for three latitudes, corresponding to beginning, middle, and end of the satellite passage. Night data were not obtained because the satellite transmitter was inoperative.

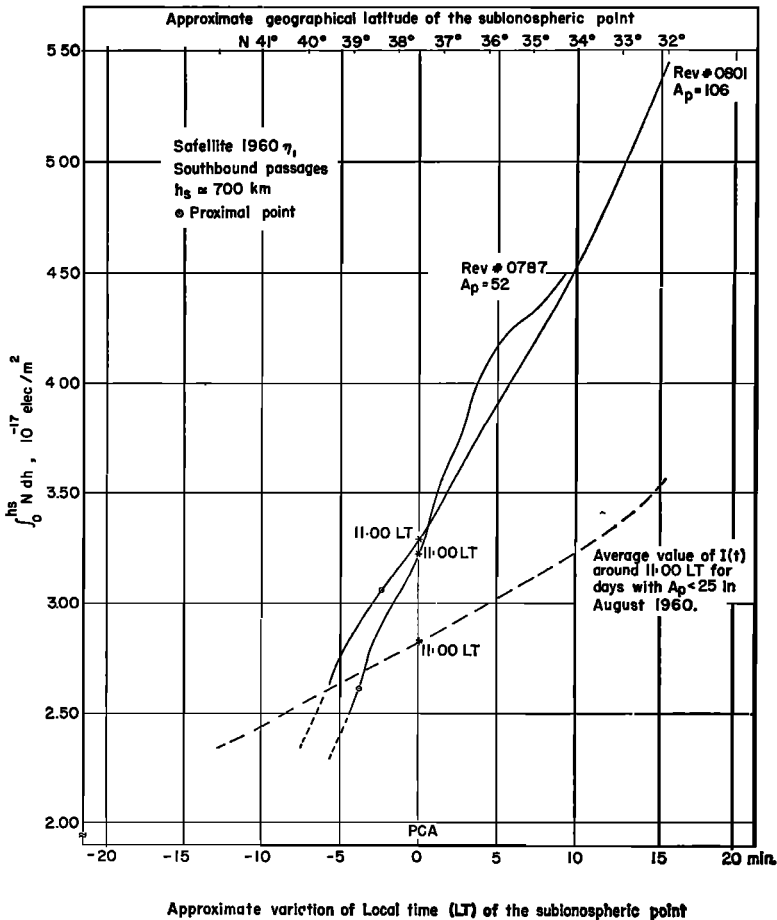


Fig. 11. Effects of the magnetic storm of August 16, 1960, on the electron content  $\int N dh$  measured in southbound passages of the satellite 1960 $\eta_1$ . Observe the substantial increase in the north-south horizontal gradient caused by a 'positive disturbance' for the lower latitudes. The broken line represents the average  $I(t)$  around noon for days with  $A_p < 25$  in August 1960.

obtained by *Garriott* [1960], *Yeh and Swenson* [1961], and *Ross* [1960] by means of observations of satellite transmissions, and by *Taylor* [1961] by means of differential Faraday fadings of lunar radio echoes, if we take into consideration their geomagnetic latitude of observation. These results also seem to support the observational results of *Maeda and Sato* [1959] concerning the behavior of  $f_oF_2$  during magnetic storms.

*Variation of  $I(t)$  through the day-night transition in quiet days.* Although the average variation of  $\int N dh$  in quiet days has been presented in the previous section (Figs. 7, 8, and 10), it is interesting to examine some of the passages that had their ray paths through the night-day transition. Consider, for instance, the north-

bound passages through sunset in September. Part of a plot of  $I(t)$  chosen as typical of this group is reproduced with some added details in Figure 14. The inflexion at the point  $P_1$  of this figure is caused by a combination of factors, among which the most preponderant is that the height of the intersection  $L$  of the ray path with the surface of the day-night transition first increased, then decreased, and finally increased again during the course of a satellite passage. This unusual situation results from the particular orbit of the satellite and the season when the observations were made. Figure 15 is a pictorial view of the geometry of this situation. Figure 16 depicts the projection of the ray on the earth for the instant of time corresponding to the

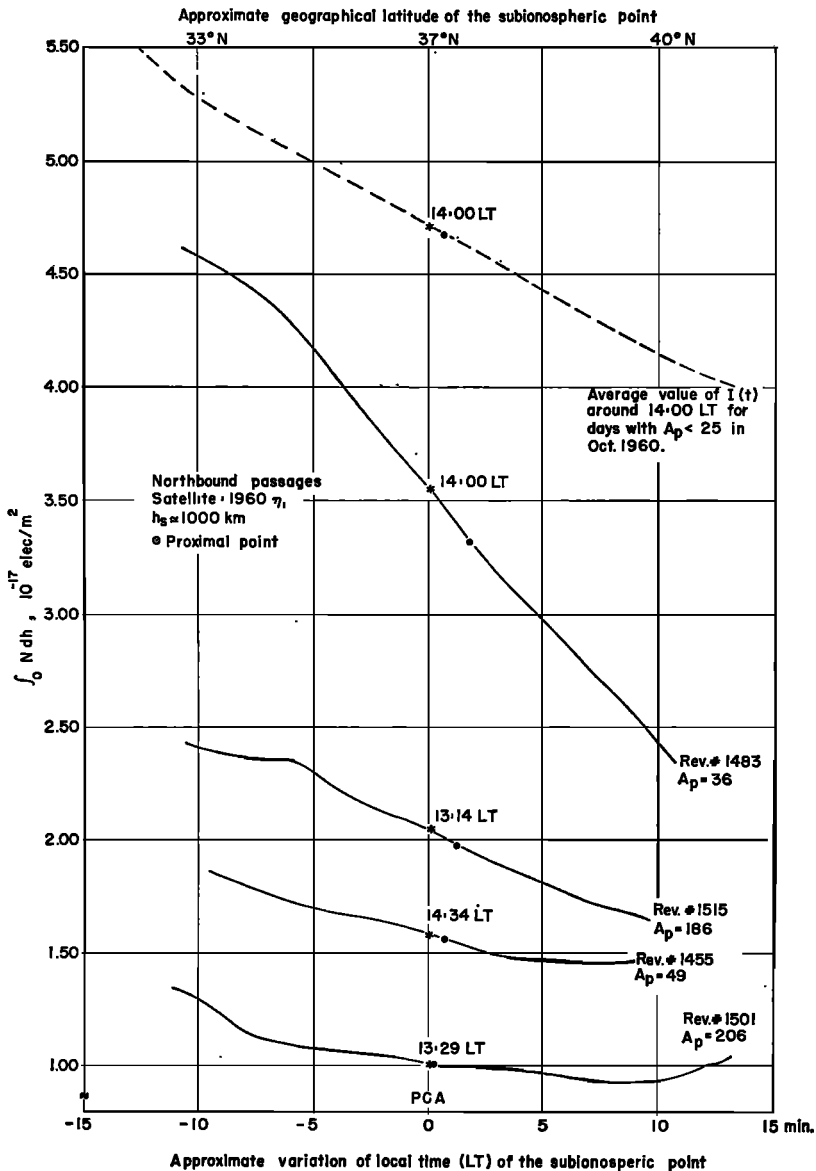


Fig. 12. Effects of the magnetic storm of October 6, 1960, on the electron content  $\int N dh$  measured in northbound passages of the satellite 1960 $\eta_1$ . Observe the increase in north-south horizontal gradient and also the greater depression of  $\int N dh$  for higher magnetic activity ( $A_p$ ).

point  $P_1$  for several passages during sunset. This sequence of passages shows a progressive situation; that is, from the passage when most of the ionosphere is in darkness (curve A) to that when most of the ionosphere is exposed to sunlight (curve F).

*Day-to-day variation of  $I(t)$ .* It was observed that most of the day-to-day variations of the

total electron content  $I(t)$  at a given hour, in magnetically quiet periods, were about 15 per cent from the mean. However, it was also observed that there were less-frequent magnetically quiet days in which  $I(t)$  varied as much as  $\pm 50$  per cent from the average. These days, unlike the magnetically disturbed, showed neither unusual variations of the equivalent

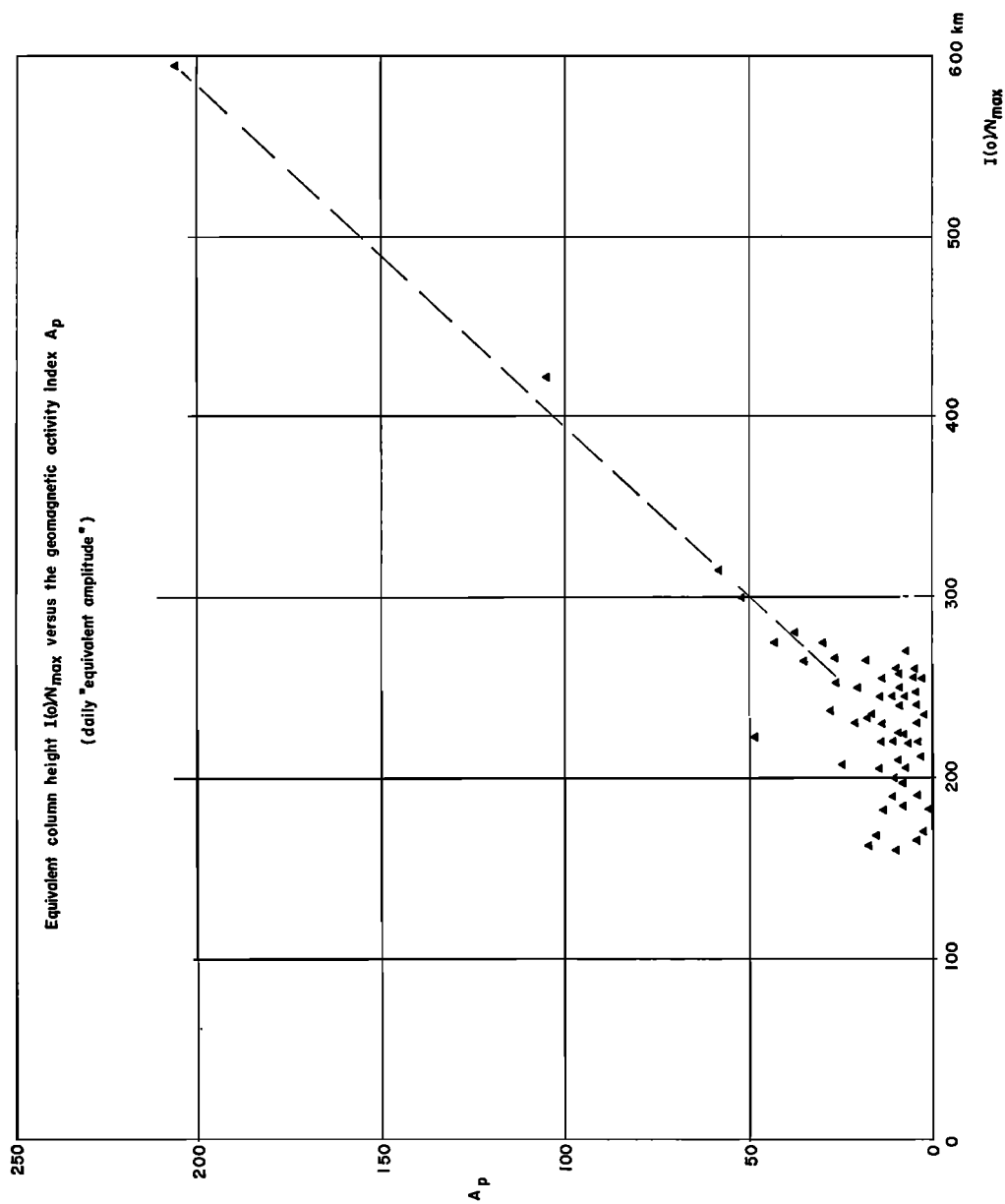


Fig. 13. Equivalent column height  $I(0)/N_{max}$  versus magnetic index  $A_p$ , for most of the satellite passages listed in Tables 1, 2, and 3.

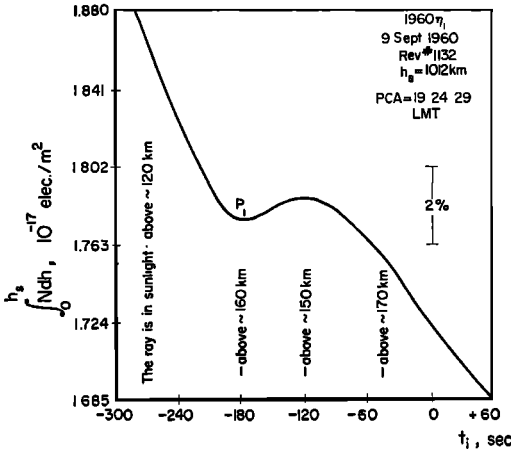


Fig. 14. Typical variation of  $I(t)$  when part of the ray path is in the sunlight. The curve  $D$  of Figure 16 depicts the subposition of the ray at  $t_i = -180$  sec.

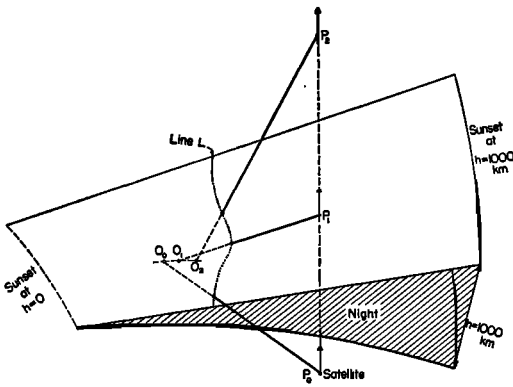


Fig. 15. Pictorial view of the intersection of the ray with the surface of the sunset transition at different times.

height  $I(0)/N_{\max}$  nor greater slopes of  $I(t)$ . This can be seen in the examples of Figure 17 for abnormally high  $I(t)$ . For abnormal decrease of  $I(t)$  the situation seemed to last longer than a day.

These day-to-day variations have been observed by other workers. *Ross* [1960] reported variations that may be as large as  $\pm 20$  per cent from the mean and remarked upon the fidelity with which they were reproduced in the lower-ionosphere data. *Yeh and Swenson* [1961] also reported large depressions of electron content during relatively quiet days. The causes of these variations are yet unknown.

*Short-time variations of  $I(t)$ .* Considering again the plots of  $I(t)$ , it could be shown that, if we were to compute an average  $\bar{I}(t)$  and form the differences  $[I(t) - \bar{I}(t)]$ , the small irregularities in electron content would become more evident [Little and Lawrence, 1960]. The presence of these irregularities can be readily detected from the curves of the Doppler shift offset ( $\Delta\dot{P}/\lambda$ ) which were concurrently plotted with  $I(t)$  for every second of the satellite passage as shown in Figures 5, 9, and 18. Irregular variations in the Doppler shift offset imply irregular variations of the phase path length  $P$  which can only be caused by nonuniform electron distribution. The heights of these irregularities cannot be determined from the present data because the satellite passages were always above 650 km; the shapes of these irregularities are also undetermined. Nevertheless, we can derive certain conclusions from the mentioned plots considering that the subionospheric point moved horizontally at an average of 3 km/sec. Since measurements were made arbitrarily at every second of a passage, the lower limit of our scale is 3 km. Small-scale irregularities of these dimensions are present in every recorded passage, either alone or within the larger irregularities. The smaller irregularities are more conspicuous after the sunrise than they are the rest of the

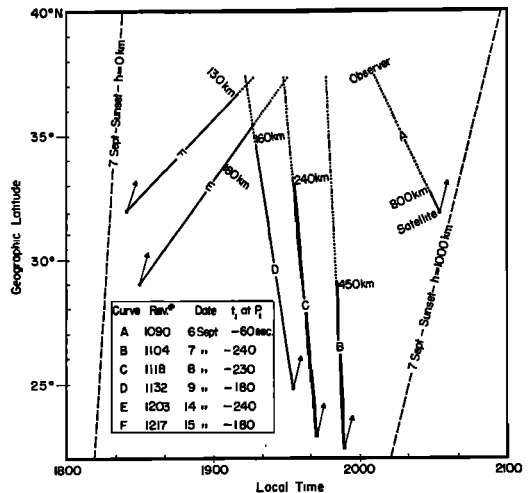


Fig. 16. Projections of the ray path on the surface of the earth for the time corresponding to the inflection points on the passages through sunset. The arrows indicate the direction of the subsatellite positions.

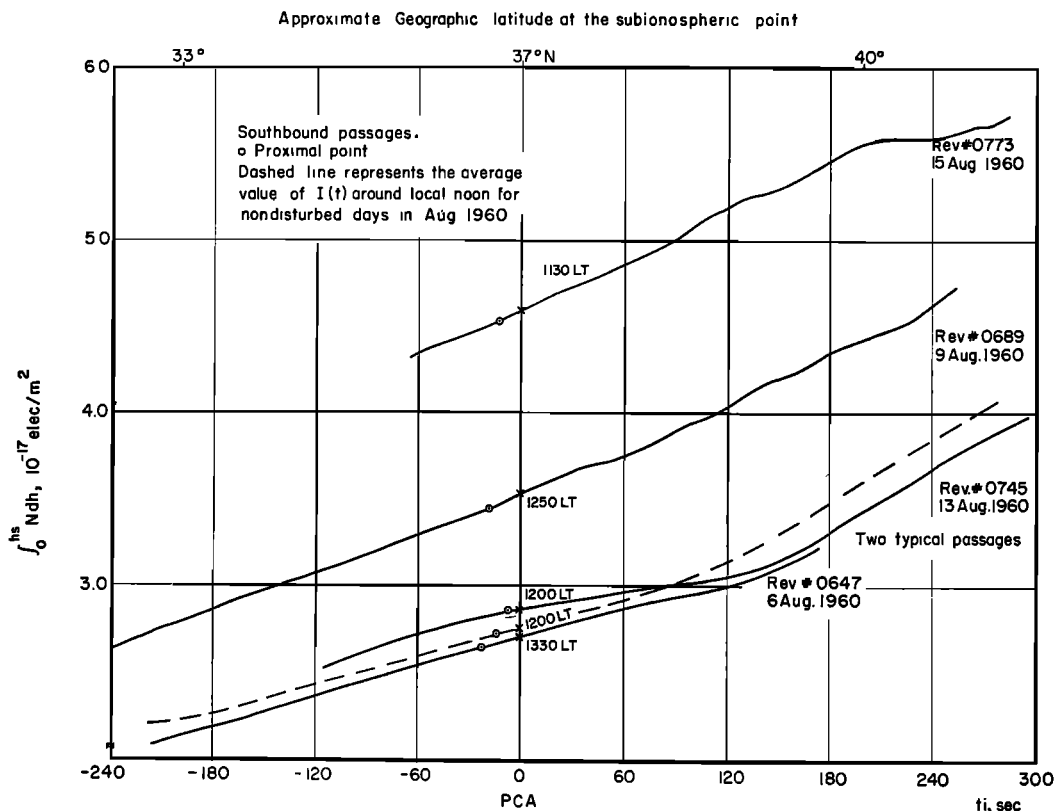


Fig. 17. Abnormally high  $I(t)$  on magnetically quiet days. Note that the slope of  $I(t)$  does not suffer major modifications.

day. Their presence does not imply the appearance of signal-amplitude fluctuations known as scintillation. There seems to be a tendency for the appearance of more irregularities for that part of the passage closer to the magnetic zenith (see, for instance, Fig. 9 at  $t_i \approx 100$  sec and Fig. 18 at  $t_i \approx -100$  sec). This fact does not imply that these clouds of electrons are localized only at the mentioned region, but simply indicates that they are aligned with the magnetic field lines.

#### CONCLUSIONS

The method developed in this paper for solving the differential equation 13 provides an accurate and relatively fast way of computing the total electron content  $I(t)$ .

Some of the results confirm and amplify the work done by other workers, but topics hitherto unreported include the marked increase of the north-south horizontal gradient of the electron

content during magnetic storms, the increase of  $\int N dh$  for lower latitudes during magnetic storms, and the day-to-day constancy of the gradient of  $I(t)$  in magnetically quiet days. The measurements of horizontal gradients also show that the common assumption of small horizontal gradients at times not close to sunrise or sunset does not seem to hold in the majority of the days, at least in the range of geomagnetic latitudes of  $35^\circ\text{N}$  to  $50^\circ\text{N}$ .

Steps are being taken to apply the method to data acquired in other satellite stations and thus increase the latitudinal range of observations with the purpose of studying the magnetic storm effects in the behavior of the ionosphere.

*Acknowledgments.* I am indebted to Dr. O. K. Garriott for guidance and many discussions, to Professor O. G. Villard, Jr., for a critical reading of the manuscript and helpful suggestions, and I also wish to thank Professors R. N. Bracewell and A. M. Peterson for their valuable comments. The equipment maintenance as well as many of the

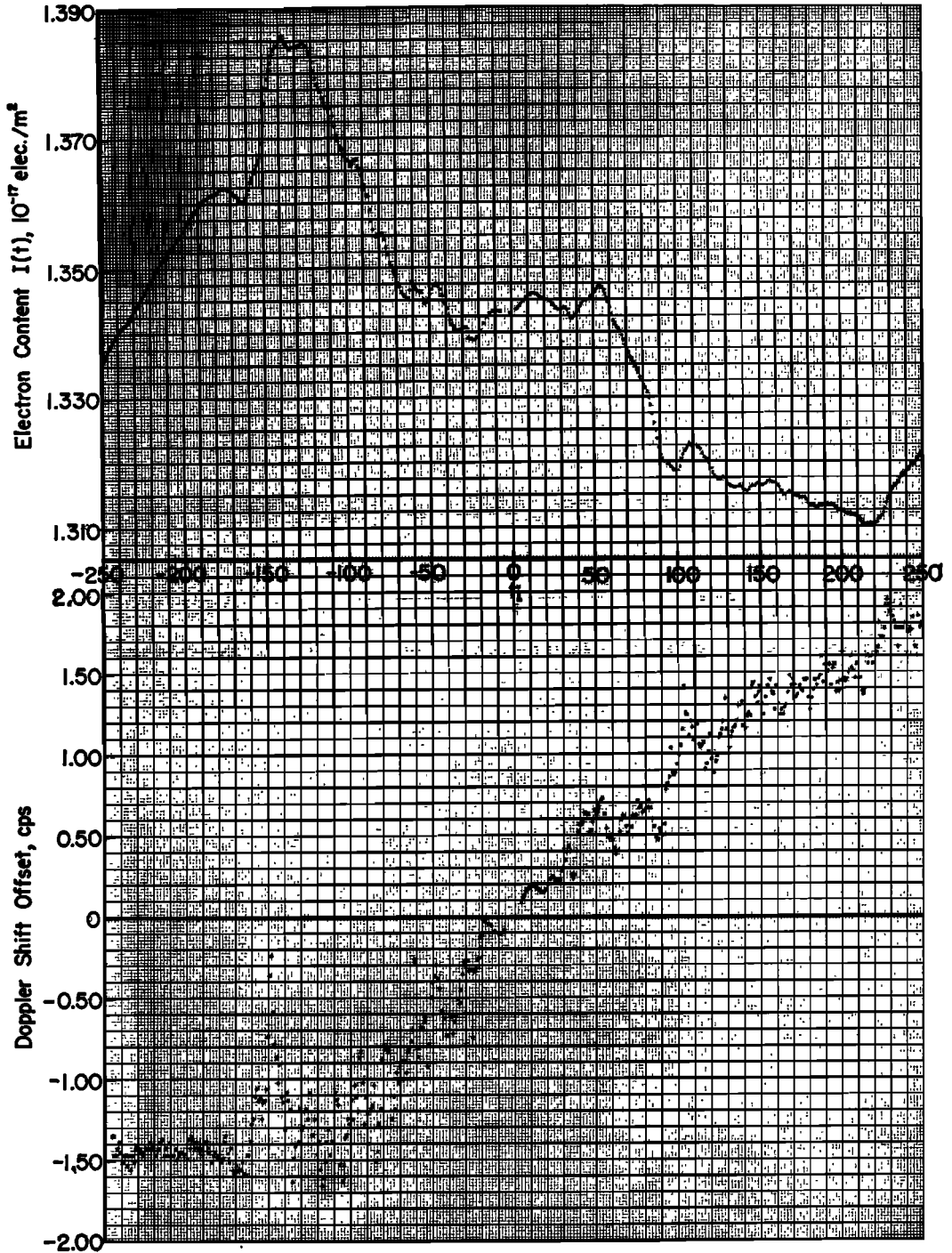


Fig. 18. Electron content and Doppler shift offset as a function of time ( $t_i$  in seconds) for a northbound passage of the satellite Transit 2-A with PCA at 06h 01m 32s (LMT) on July 28, 1960. Small-scale irregularities in the electron distribution causes the scattering of the points in the Doppler shift offset curve with corresponding variations in  $I(t)$ .

data recordings were handled by Mr. S. C. Hall. A considerable amount of time was spent on data reduction by Mr. P. Whitehead, Mrs. L. Ebner, and Mr. K. Byram. The extensive programming for the computer was performed by Mr. D. Westover. Without such a large amount of cooperation from these individuals and other members of this Laboratory, the report could not have been completed. The microfilmed ephemerides for the satellite 1960 $\eta_1$  were forwarded to us by Dr. G. C. Weiffenbach of the Johns Hopkins University, whose cooperation has been very helpful.

I am on leave from the Brazilian Air Force and have been supported partly by a grant from the Brazilian Government through its Campanha Nacional de Aperfeiçoamento de Pessoal de Nível Superior. Financial support for the work presented here has been provided by the National Aeronautics and Space Administration under grant number NSG-30-60.

## REFERENCES

- Aitchison, G. J., and K. Weekes, Some deductions of ionospheric information from the observations of emissions from satellite 1957 $\alpha_2$ , 1, *J. Atmospheric and Terrest. Phys.*, 14, 236-243, 1959.
- de Mendonça, F., and O. K. Garriott, Ionospheric electron content calculated by a hybrid Faraday-Doppler technique, submitted for publication in *J. Atmospheric and Terrest. Phys.*, 1962a.
- de Mendonça, F., and O. K. Garriott, The effect of the earth's magnetic field on measurements of the Doppler shifts of satellite radio transmissions, *J. Geophys. Research*, 67(5), 1962b.
- Garriott, O. K., The determination of ionospheric electron content and distribution from satellite observations, 1 and 2, *J. Geophys. Research*, 65, 1139-1157, 1960.
- Garriott, O. K., and R. N. Bracewell, Satellite studies of the ionization in space by radio, in *Advances in Geophysics*, 8, 85-135, Academic Press, New York, 1961.
- Garriott, O. K., and A. W. Nichol, Ionospheric information deduced from the Doppler shifts of harmonic frequencies from earth satellites, *J. Atmospheric and Terrest. Phys.*, 22(1), 50-63, 1961.
- Hibberd, F. H., and J. A. Thomas, The determination of electron distribution in the upper ionosphere from satellite Doppler observations, *J. Atmospheric and Terrest. Phys.*, 17½, 71-81, 1959.
- Little, C. G., and R. S. Lawrence, The use of polarization fading of satellite signals to study the electron content and irregularities in the ionosphere, *J. Research NBS*, 64D, 4, 1960.
- Maeda, K. I., and T. Sato, The F region during magnetic storms, *Proc. IRE*, 47, 232-239, 1959.
- Nisbet, J. S., and S. A. Bowhill, Electron densities in the F region of the ionosphere from rocket measurement, 1 and 2, *J. Geophys. Research*, 65(11), 3601-3614, 1960.
- Ratcliffe, J. A., *The Magneto-Ionic Theory and Its Applications to the Ionosphere*, Cambridge University Press, pp. 75-77, 1959.
- Ross, W. J., The determination of ionospheric electron content from satellite Doppler measurements, 1 and 2, *J. Geophys. Research*, 65(9), 2601-2615, 1960.
- Seddon, J. C., Propagation measurements in the ionosphere with the aid of rockets, *J. Geophys. Research*, 58(3), 323, 1953.
- Taylor, G. N., The total electron content of the ionosphere during the magnetic disturbance of November 12-13, 1960, *Nature*, 189(4766), 740-741, 1961.
- Weekes, K., On the interpretation of the Doppler effect from senders in an artificial satellite, *J. Atmospheric and Terrest. Phys.*, 12, 335, 1958.
- Yeh, K. C., and G. W. Swenson, Jr., Ionospheric electron content and its variations deduced from satellite observations, *J. Geophys. Research*, 66, 1061-1067, 1961.

(Manuscript received January 15, 1962;  
revised March 8, 1962.)